



Effect of low processing rate on homogeneous microstructural evolution of polyacrylonitrile-based carbon fibers

Doo-Won Kim¹ · Dae Ho Kim² · Sung Ryong Kim² · Bo-Hye Kim³ · Yun Hyuk Bang⁴ · Duck Joo Yang⁵ · Go Bong Choi⁶ · Yoong Ahm Kim⁶ · Kap Seung Yang^{6,7}

Received: 30 October 2018 / Accepted: 21 January 2019 / Published online: 21 May 2019
© Korean Carbon Society 2019

Abstract

This study demonstrates that low processing rate for producing polyacrylonitrile (PAN)-based carbon fiber is a critical to obtain a homogeneous radial microstructure with high resistance to oxidation, thereby resulting in their improved mechanical strength. The dry-jet wet spun PAN organic fibers were processed (e.g., stabilized and then carbonized) utilizing two different rates; one is 1.6 times longer than the other. The effect of processing rate on the microstructural evolutions of carbon fibers was analyzed by scanning electron microscopy after slow etching in air, as well as Raman mapping after graphitization. The rapidly processed fiber exhibited the multilayered radial structure, which is caused by the radial direction stretching of the extrusion in the spinning. In case of the slowly processed fiber, the layered radial structure formed in the spinning process was changed into a more homogeneous radial microstructure. The slowly processed fibers showed higher oxidation resistance, higher mechanical properties, and higher crystallinity than the rapidly processed one. Raman mapping confirmed that the microstructure developed during spinning was sustained even though fiber was thermally treated up to 2800 °C.

Keywords Carbon fibers · Microstructure · Mechanical properties · Oxidation · Polyacrylonitrile · Carbonization

1 Introduction

Carbon fiber-reinforced plastics (CFRPs) have received much attention in recent years as a result of their excellent mechanical, thermal, and physical properties [1, 2]. These excellent properties allow for the use of CFRPs in aeronautics, aerospace, sporting goods, and leisure industries [3–5].

Commercially available polyacrylonitrile (PAN)-based CFs are normally produced in two continuous processes. The first process involves wet- or dry-jet wet spinning of PAN, which includes a spray wash, boiling water stretch (2–6 times), and packing. The second process includes steam stretching, followed by oxidative stabilization (200–300 °C), first carbonization (500–1000 °C), and second carbonization (~1500 °C). The structure of the CF, including defects, is strongly dependent upon all processing parameters. CFs' defects normally originate from impurities, gels in the

Electronic supplementary material The online version of this article (<https://doi.org/10.1007/s42823-019-00047-7>) contains supplementary material, which is available to authorized users.

✉ Yoong Ahm Kim
yak@chonnam.ac.kr

✉ Kap Seung Yang
ksyang@chonnam.ac.kr

¹ Institute of Advanced Composite Materials, Korea Institute of Science and Technology, 92 Chudong-ro, Bongdong-eup, Wanju-Gun, Jeonbuk 55324, Republic of Korea

² Hyosung Corporation, Jeonju Plant, 886 Girin-daero, Deokjin-gu, Jeonju-Si, Jeonbuk 54849, Republic of Korea

³ Division of Science Education, Chemistry Education Major, Daegu University, 201 Daegudae-ro, Gyeongsan-Si, Gyeongsangbuk-do 38453, Republic of Korea

⁴ Korea Institute of Carbon Convergence Technology, 110-11 Banlyong-ro, Deokjin-gu, Jeonju-si, Jeollabuk-do 54853, Republic of Korea

⁵ Department of Chemistry, University of Texas at Dallas, 800 West Campbell Rd, Richardson, TX 75080, USA

⁶ Department of Polymer Engineering, Graduate School, School of Polymer Science and Engineering and Alan G. MacDiarmid Energy Research Institute, Chonnam National University, 77 Yongbong-ro, Buk-gu, Gwangju 61186, Republic of Korea

⁷ Carbon Composite Materials R&D Center HPK Inc, 308 Venture Support Building, Banlyong-ro, Deokjin-gu, Jeonju-Si, Jeollabuk-do 54853, Republic of Korea

solution, solvent–non-solvent exchange during coagulation, the viscosity gradient during the stretching process, and/or heterogeneous structure formation during stabilization and carbonization [6–8].

A multilayered radial structure was evolved during fiber stretching as a result of viscosity variations in the radial direction [9]. Actually, the radial coagulation gradient was generated as a result of non-solvent diffusion from the fiber skin to fiber core. A small radial gradient between the skin and core brings about a relative viscosity difference, then leading to a radial distribution of tensile stress. The distribution of stress along the filament radius introduced a microstructural gradient consisting of a highly ordered structure at the skin and less ordered structure at the core. While stretching introduces a highly ordered structure at the skin, severe stretching creates defects on the skin, thereby weakening the mechanical properties of the fibers.

Defects generated within CFs are known to diffuse onto the surface when CFs are exposed to various processes, thus leading to large surface areas, which allow for reactions with oxygen. It is well known that the oxidation resistivity of CFs is closely related to their microstructure [10, 11]. Yang et al. revealed that high modulus CFs, such as PAN- and pitch-based CFs, exhibited a high oxidation resistivity owing to their relatively high crystallinity. Therefore, it is essential to understand how various processing parameters (e.g., such as spinning, stabilization, and carbonization) are related to their microstructures as well as their mechanical properties.

In this study, we systematically elucidated the oxidation behavior and mechanical properties of PAN-based CFs related to their microstructure as a function of processing rate (controlled by retention time). The relative processing rates chosen were rapid process (RP), as a control, and slow process (SP), which was 1.6 times longer than in the RP process. The microstructure was analyzed by scanning electron microscopy (SEM) after slow etching in air at 580 °C, and Raman mapping was obtained after graphitization. Both samples were comparatively characterized in terms of their crystallinity, density, and mechanical properties.

2 Experimental

2.1 Preparation of carbon fibers

The carbon filaments were prepared via the dry-jet wet spinning of PAN copolymer in dimethyl sulfoxide (DMSO) on a pilot scale, capable of producing 100 kg/day of PAN precursor fiber. The PAN fibers were processed continuously through oxidative stabilization and carbonization, up to 1400 °C. To elucidate the effect of processing rate on the microstructure, two process rates were chosen. The RP samples were stabilized at 2.5 °C/min and carbonized at 300 °C/

min. The SP samples were obtained using 1.6 times slow rate. The details of the PAN copolymer composition and other process conditions were difficult to open because of their commercial processes. Here, T700-grade CF (Toray, PAN-based CF), which has been widely used for CFRP, was chosen as a reference for comparison.

2.2 Etching by oxidation and graphitization

To examine the radial microstructure, the CFs were chopped into 3–4-mm-length segments, placed in a tubular furnace, and heated to 580 °C at 20 °C/min under nitrogen flow (50 mL/min). Upon reaching 580 °C, the samples were oxidized by shifting from nitrogen to air flow (50 mL/min) for 130 min. To observe the morphology of the longitudinal fiber surface, the long fibers were loaded into the tubular furnace, with one side fixed and the other loaded with a weight during thermal treatment. The long carbon filaments were oxidized in the same manner as the chopped CFs except that, for the long carbon filaments, the 50 mL/min air flow was performed at 500 °C (as opposed to 580 °C for the chopped fibers), and held for 5, 10, 15, and 20 h. The oxidation yield of CFs was obtained by dividing the weight of the oxidized sample by that of the pristine. The detailed experimental schematic diagram is shown in Fig. S1. Finally, the carbonized samples were graphitized by heating up to 2000 °C at 20 °C/min and to 2800 °C at 5 °C/min, followed by a 30-min isotherm and natural cooling using a graphite furnace in an argon atmosphere.

2.3 Characterization

The surface morphologies of the CF samples were observed using a Hitachi scanning electron microscope (S-4700, Hitachi). The crystalline structures of the CF samples were analyzed by an X-ray diffractometer (D-Max-2400 diffractometer) with CuK α radiation ($\lambda = 0.15418$ nm). The crystallite height (L_c) was determined via the Scherrer equation [12]. We obtained Raman spectra using a 533-nm Ar-ion laser (inVia confocal Raman microscope with streamline option, Renishaw, UK) and then calculated R value (I_D/I_G , the integrated peak intensity of the D-band divided by the integrated intensity of the G-band). Raman mapping was obtained by dividing target area into square with unit of 188 pixels per inch (ppi), and then, the R value was obtained from each square. The density measurement was taken using a density gradient column (Polytest, RayRan, UK). The mechanical properties of the CFs were measured by a mechanical tester for single filaments (FAVIMAT+, Tex-techno, Germany), with a test speed of 2 mm/min and gauge length of 25 mm. The data collected from 20 specimens for each CF sample were averaged. The electrical resistivity of

single carbon filaments was evaluated using the four-point probe method with 500 μm separation between the probes.

3 Results and discussion

3.1 Cross-sectional microstructure

The development of a multilayered radial structure in the stretching step occurs due to a viscosity variation in the radial direction. Basically, the radially developed structure is not largely changed through the stabilization and following carbonization processes. Figure 1 shows the cross-sectional SEM images of the pristine and chopped CFs etched by oxidation. The etched surface allows us to visualize the cross-sectional microstructure with radially developed multilayered structures for both T700 and RP samples (Fig. 1d, f). It is reported that lower crystallinity regions can be etched earlier in the oxidation process than higher crystallinity regions [13, 14]. Thus, it is possible to say that the multilayered structure having

different crystallinities was generated in the stretching process of the spinning step due to high viscosity gradient at the skin of the gel fiber. Consequently, the radially developed microstructure in the RP sample was sustained through thermal treatment [15]. On the contrary, the SP sample does not exhibit the multilayered radial structure, indicating that the heterogeneous structure formed in the spinning process was homogenized by slow stabilization and carbonization (longer retention time).

The oxidation yields for T700, SP, and RP were 74.3, 72.4, and 50.3%, respectively, as summarized in Table 1. Previous reports found that the CF core possessed a less crystalline structure [15, 16]. The T700 and RP samples acquired a pleat-like microstructure on the fiber surface when the diameter is reduced to 5 μm by oxidation. On the other hand, the SP sample showed no significant variation in the microstructure from the core to skin (Fig. 1e), representing no significant variations in crystallinity. From these observations, it can be concluded that the SP sample is more crystalline than both the T700 and RP samples.

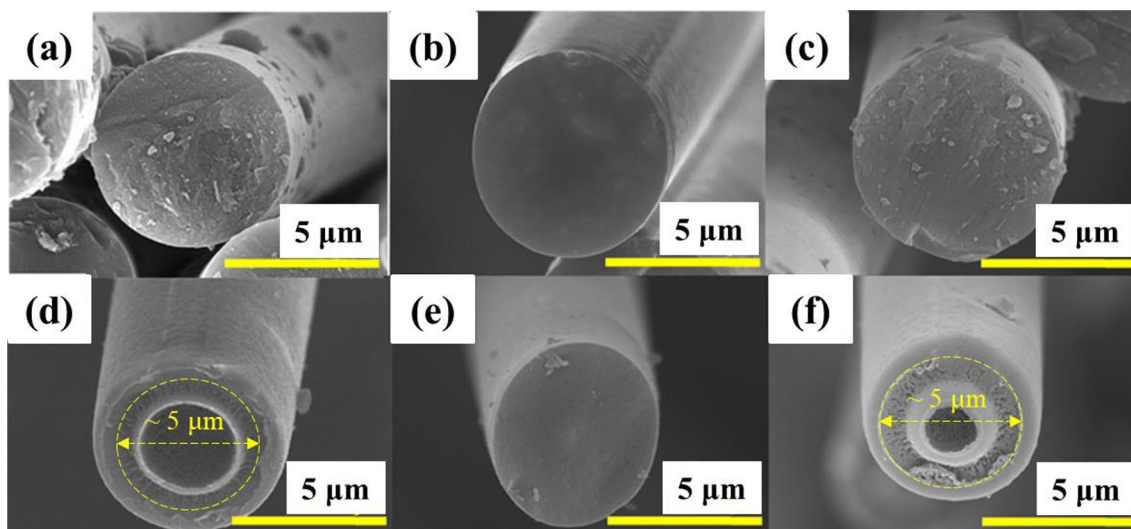


Fig. 1 Cross-sectional SEM images of pristine. **a** T700, **b** SP, and **c** RP, and oxidized at 580 $^{\circ}\text{C}$ for 130 min, **d** T700, **e** SP, and **f** RP

Table 1 Basic properties of chopped and long CFs before and after the 20-h oxidation

	Chopped CFs	Carbon filament			
		Before oxidation		After the 20-h oxidation	
	Yield of chopped CFs after oxidation (%)	Diameter of pristine CFs (μm)	FWHM of pristine CFs at 26° in XRD pattern ($^{\circ}$)	Diameter of 20-h oxidized CFs (μm)	FWHM of 20-h oxidized CFs at 26° in XRD pattern ($^{\circ}$)
T700	74.3	7.0	5.44	5.3	6.80
SP	72.4	6.8	4.94	5.4	4.96
RP	50.3	6.8	5.67	3.9	6.46

3.2 Longitudinal surface of carbon filament

Figure 2 illustrates the yield of the carbon filaments depending on oxidation time. All carbon filament samples showed high oxidation resistance until 5 h (yield of over 90%). The RP sample showed a rapid decrease in yield with oxidation time after 5 h. On the other hand, T700 and SP samples showed similar yields until 15 h. The SP sample produced higher yields than T700 at 20 h.

Figure 3 shows the CF surface microstructure as a function of oxidation time. Both RP and T700 samples had a smooth surface while being etched up to 15 h, and a pleat-like surface structure at 20 h. This represents a heterogeneous radial morphology, with a more crystalline skin structure and less ordered core. In contrast, the yield of the RP sample rapidly is decreased with increasing oxidation time. The results illustrate that both T700 and RP samples exhibit similar radial structures, while the oxidation resistivity was slightly higher for T700 compared with the RP sample, indicating the presence of more defects in the RP sample. However, the SP sample possessed a smooth surface and slow diameter reduction even after a 20-h oxidation.

3.3 Microstructure of the carbon filament

To evaluate crystallite thickness (L_c) in the carbon filaments, XRD patterns were obtained (Fig. 4). All pristine T700 and RP samples showed similar XRD patterns consisting of a broad peak from $2\theta = 20^\circ - 30^\circ$ (Fig. 4a). The average crystallinities of the RP and T700 samples are not significantly different because they have presumably similar processing conditions [17, 18]. However, pristine SP showed a smaller full-width-at-half-maximum (FWHM) value at 26° (Table 1), indicating a more ordered crystalline structure than the two other CFs. After the 20-h oxidation,

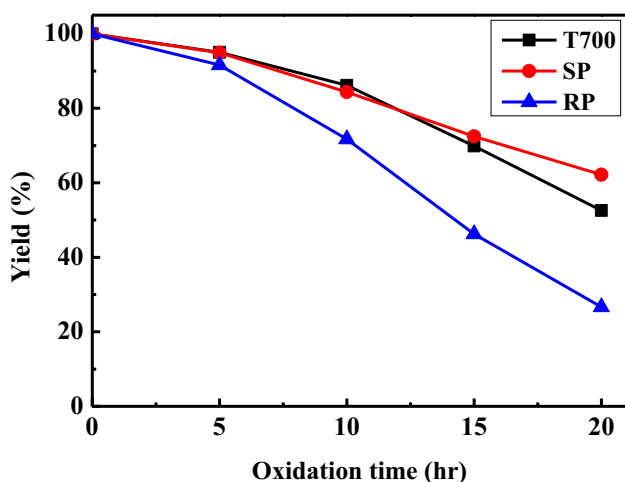


Fig. 2 Yield of carbon filaments as a function of oxidation time

XRD patterns of RP and T700 samples showed significantly broadened peaks, presented by a FWHM at 26° (Fig. 4b; Table 1). On the other hand, the SP sample showed almost no change in the FWHM value at 26° or L_c values after the 20-h oxidation (Fig. 4c). These behaviors reflect the radially developed microstructure. For example, RP and T700 samples have a clear radial structure with a more crystalline skin and less crystalline core [19, 20]. On the other hand, the SP sample showed the highest L_c value for both pristine and 20-h oxidation samples, even sustaining the original value. This indicates that the SP sample has a homogeneous radial microstructure, with high crystallinity, resulting in a high oxidation resistivity.

Raman mapping was performed to observe the structural perfection of the graphitized fibers at 2800°C . In Fig. 5, the microstructures of the graphitized carbon filaments are compared using Raman mapping images of the fiber cross sections. The full width at half maximum (FWHM) of the G-band [21] and R value (I_D/I_G) of the CFs [22] were compared in order to visualize variations in the degrees of crystallinity. The distinctive difference is clearly observed from R value for three samples.

Both data indicated that the crystallinity of graphitized T700 and RP samples was lower in the core than in the skin. Specifically, T700 CFs showed a higher oxidation resistivity than the RP samples presumably as a result of more defects in the RP sample. The defects are coming from impurities, gels in the solution, solvent–non-solvent exchange during coagulation, the viscosity gradient in the stretching process, and heterogeneous structure formation during stabilization and carbonization [23, 24]. On the other hand, the graphitized SP sample possessed uniform crystallinity over the whole cross section. Despite the SP and RP samples being manufactured under the same conditions, except for the retention time at stabilization and subsequent carbonization, both showed differing crystallinity at graphitization temperature. Raman mapping confirmed that the microstructure formed at an early stage was sustained even upon graphitization at 2800°C . We therefore deduced that a high oxidation resistivity and a highly crystalline microstructure of the CFs can be obtained via homogeneous stabilization via cyclization and cross-linking reactions [25, 26]. Homogeneous stabilization with increased retention time minimized the effects of radial structural variations (which are formed during the solution spinning process) after thermal treatment at 1400°C . Moreover, in the carbonization process, a multitude of defects originating from insufficient cross-linking led to a low oxidation resistivity.

3.4 Physical and mechanical properties of the CFs

In Table 2, the densities, mechanical properties, and electrical resistivities of the single carbon filaments are

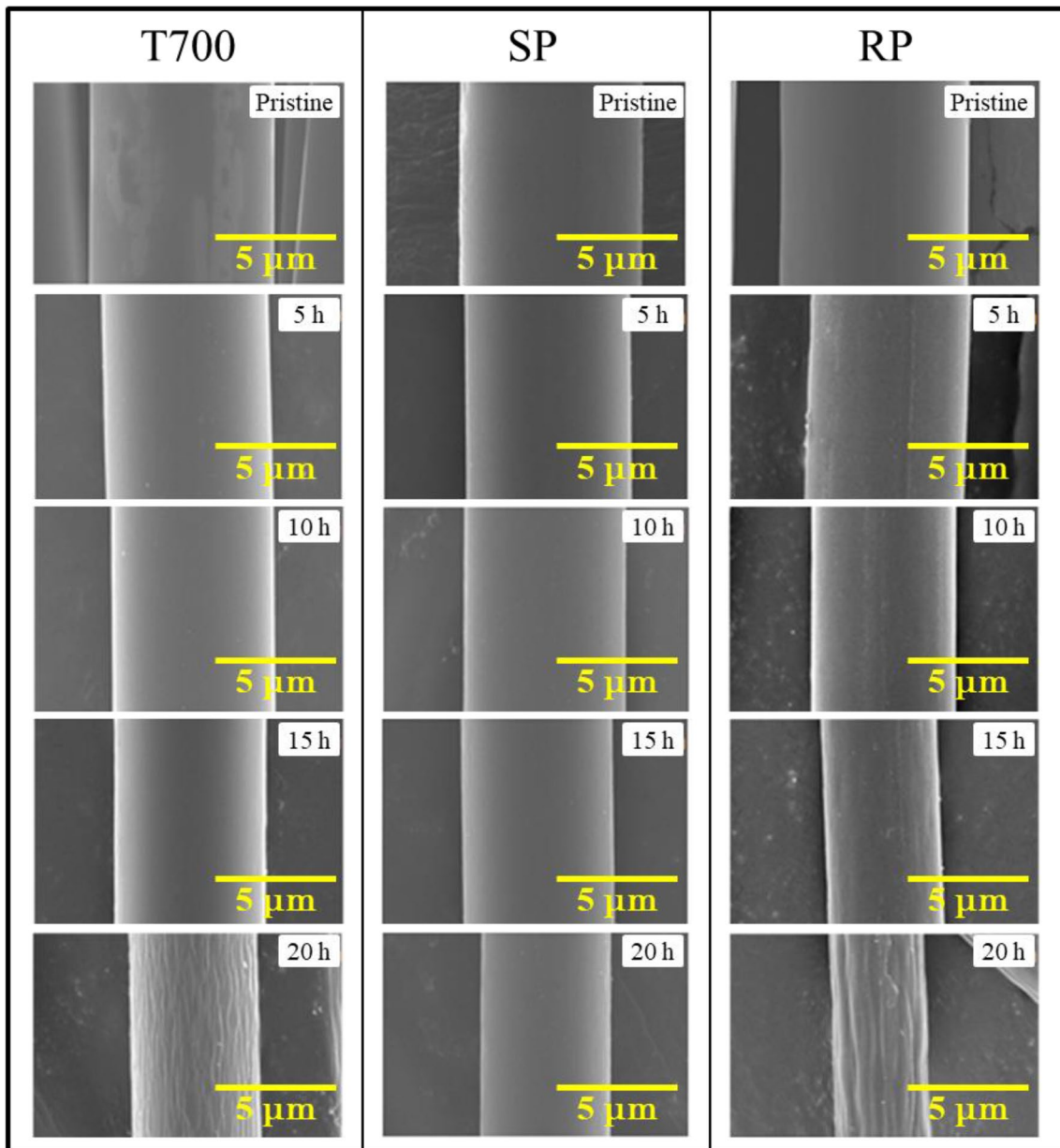


Fig. 3 SEM images of pristine and oxidized carbon filaments as a function of oxidation time

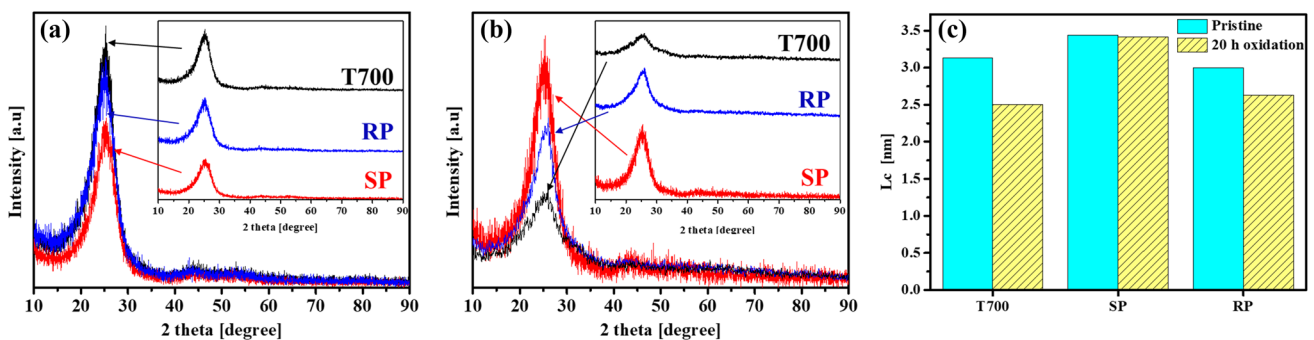


Fig. 4 X-ray diffraction patterns of **a** pristine carbon filaments, **b** 20-h oxidized CFs, and **c** their calculated L_c values

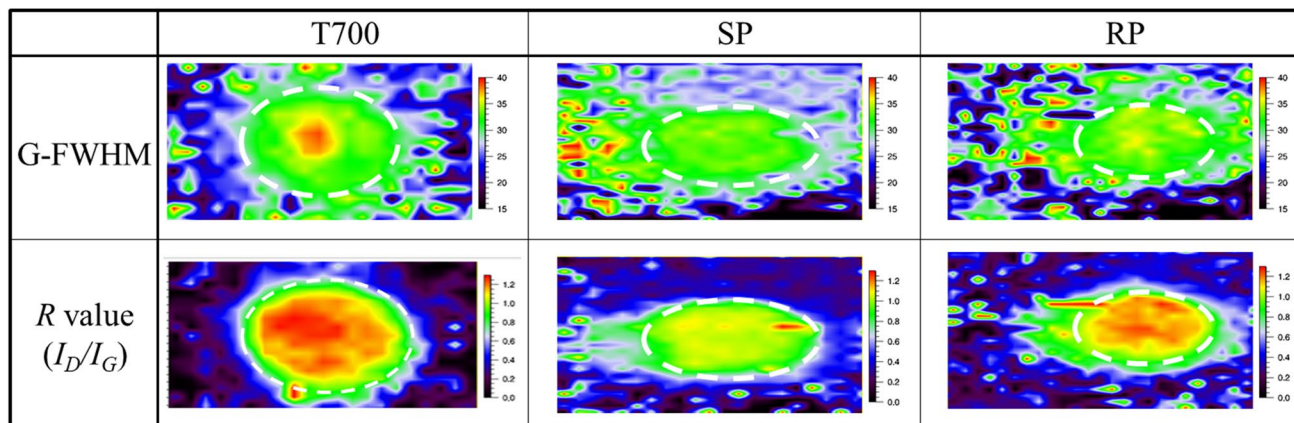


Fig. 5 Cross-sectional Raman mapping images of the thermally treated carbon fibers at 2800 °C in argon. G-FWHM is the full width at half maximum of the G-band, and R value (I_D/I_G) is the integrated intensity of the D-band divided by the integrated intensity of the G-band

Table 2 Physical and mechanical properties before and after the 20-h oxidation

	Before oxidation				After the 20-h oxidation			
	Density (g/cm)	Tensile strength (GPa)	Tensile modulus (GPa)	Electrical resistivity (mΩ-cm)	Density of 20-h oxidized CFs (g/cm)	Tensile strength (GPa)	Tensile modulus (GPa)	Electrical resistivity (mΩ-cm)
T700	1.80	3.75	240.3	1.99 ± 0.05	1.84	2.81	244.1	2.34 ± 0.19
SP	1.78	4.13	281.1	1.72 ± 0.12	1.79	3.25	302.9	1.58 ± 0.16
RP	1.79	3.49	257.0	2.00 ± 0.16	1.85	2.35	204.2	2.02 ± 0.08

summarized for the pristine and 20-h oxidation samples. Pristine T700, RP, and SP samples possessed densities of 1.80, 1.79, and 1.78 g/cm, respectively. After the 20-h oxidation, the densities of all samples increased, and the increment was in the order of RP (0.06 g/cm) > T700 (0.04 g/cm) > SP (0.01 g/cm). The density variations after oxidation originate from changes in the proportions of the crystalline and amorphous regions. The RP and T700 samples consist of distinct crystalline and amorphous regions. The amorphous region would be etched more quickly compared to the crystalline region, resulting in density enhancements after oxidation. On the other hand, the SP sample, possessing a homogeneous radial structure, showed almost no change in the density.

The pristine single carbon filament of the SP sample showed the highest tensile strength at 4.13 GPa, which is 1.10 times higher than that of T700 (3.75 GPa) and 1.18 times higher than that of the RP sample (3.49 GPa). After the 20-h oxidation, although the tensile strengths of all samples decreased, the SP sample still showed the highest tensile strength (3.25 GPa), which was 1.16 times higher than that of the 20-h oxidized T700 (2.81 GPa) and 1.38 times higher than that of the 20-h oxidized RP sample (2.35 GPa). The tensile modulus of the SP sample also showed highest values for both pristine and 20-h oxidation. After oxidation, the RP

sample decreased in tensile modulus, similar to T700. After oxidation, the SP sample experienced an 8% increase in tensile modulus, which is attributed to an increase in structural perfection by oxidation under tension. The electrical resistivity also reflects the microstructure and crystallinity. Oxidation decreased the electrical resistivity of the SP sample due to the achievement of structural perfection (Table 2). On the contrary, RP and T700 samples experienced a slightly increased electrical resistivity after oxidation due to defects introduced to the less crystalline regions.

4 Conclusions

The effect of the processing rate on the microstructure of CFs was studied by controlling the retention time. The SP sample, which was processed (e.g., stabilized and carbonized) 1.6 times longer than the RP sample in a continuous commercial process, showed a higher oxidation resistivity, better mechanical properties, and a more homogeneous radial microstructure with higher crystallinity. On the other hand, the RP sample exhibited a lower oxidation resistivity and poorer mechanical properties because of their multilayered radial structure originally induced by stretching during wet spinning. Raman mapping confirmed that the

microstructure formed during lower temperature processing was sustained, even at 2800 °C. We deduced that a high oxidation resistivity, strong mechanical properties, and a highly crystalline microstructure of the CFs can be obtained by extending the processing time via adequate cyclization and cross-linking reactions. The homogeneous structure development at longer retention times minimized radial structural variations, which is originally formed in the solution spinning process. This research indicates that lower processing rates during stabilization and carbonization lead to fibers with a more homogenous microstructure, which are more resistive to oxidation. It is noteworthy that the developed microstructure at stabilization and carbonization processes is sustained after graphitization at 2800 °C.

Acknowledgements This research was supported by the Hyosung Corporation, Basic Science Research Program, through the National Research Foundation of Korea (NRF) funded by the Ministry of Education (NRF-2018R1D1A1A02046116) and Nano Material Technology Development Program through the National Research Foundation of Korea (NRF) funded by Ministry of Science and ICT (NRF-2016M3A7B4905618). Y.A.K. acknowledged the financial support from the Technology Innovation Program (20000207) funded by the Ministry of Trade, Industry & Energy (MOTIE, Korea).

References

- Gadiou R, Serverin S, Gibot P, Vix-Guterl C (2008) The synthesis of SiC and TiC protective coatings for carbon fibers by the reactive replica process. *J Eur Ceram Soc* 28(11):2265–2274
- Gao P, Wang H, Jin Z (2004) Study of oxidation properties and decomposition kinetics of three-dimensional (3-D) braided carbon fiber. *Thermochim Acta* 414(1):59–63
- Gupta A, Paliwal D, Bajaj P (1991) Acrylic precursors for carbon fibers. *J Macromol Sci Part C Polym Rev* 31(1):1–89
- Serkov A, Budnitskii G, Radishevskii M, Medvedev V, Zlatoustova L (2003) Improving carbon fibre production technology. *Fibre Chem* 35(2):117–121
- Perepelkin K (2003) Oxidized (cyclized) polyacrylonitrile fibres—oxypan. A review. *Fibre Chem* 35(6):409–416
- Donnet JB, Bansal RC (1998) Carbon fibers. CRC Press, Boca Raton
- Kelly V (2004) Carbon fiber: manufacture and applications. Elsevier, Amsterdam
- Rahaman MSA, Ismail AF, Mustafa A (2007) A review of heat treatment on polyacrylonitrile fiber. *Polym Degrad Stab* 92(8):1421–1432
- Ziabicki A, Kawai H (1985) High-speed fiber spinning: science and engineering aspects. Wiley, New York
- Zielke U, Hüttinger K, Hoffman W (1996) Surface-oxidized carbon fibers: I. Surface structure and chemistry. *Carbon* 34(8):983–998
- Jones L, Thrower P (1991) Influence of boron on carbon fiber microstructure, physical properties, and oxidation behavior. *Carbon* 29(2):251–269
- Kercher AK, Nagle DC (2003) Microstructural evolution during charcoal carbonization by X-ray diffraction analysis. *Carbon* 41(1):15–27
- Kim DH, Kim B-H, Yang KS, Bang YH, Kim SR, Im HK (2011) Analysis of the microstructure and oxidation behavior of some commercial carbon fibers. *J Korean Chem Soc* 55(5):819–823
- Matsumoto T, Mochida I (1993) Oxygen distribution in oxidatively stabilized mesophase pitch fiber. *Carbon* 31(1):143–147
- Blanco C, Lu S, Appleyard S, Rand B (2002) Micro-thermal analysis as a technique for in situ characterisation of the softening behaviour of the isotropic phase and mesophase in thermally treated pitches. *Carbon* 40(1):132–135
- Roh J-S, Kim S-H (2009) Structural study of the oxidized high modulus carbon fiber using laser Raman spectroscopy. *Carbon Lett* 10(1):38–42
- Wang S, Chen Z-H, Ma W-J, Ma Q-S (2006) Influence of heat treatment on physical–chemical properties of PAN-based carbon fiber. *Ceram Int* 32(3):291–295
- Vázquez-Santos MB, Geissler E, László K, Rouzaud J-N, Martínez-Alonso A, Tascón JM (2011) Comparative XRD, Raman, and TEM study on graphitization of PBO-derived carbon fibers. *J Phys Chem C* 116(1):257–268
- Lee Y-J, Radovic LR (2003) Oxidation inhibition effects of phosphorus and boron in different carbon fabrics. *Carbon* 41(10):1987–1997
- Lee Y-J (2004) The second order Raman spectroscopy in carbon crystallinity. *J Nucl Mater* 325(2–3):174–179
- Yoshida A (2006) Full width at half maximum intensity of G band in first order Raman spectrum of carbon material as a parameter for graphitization. *TANSO* 221:2–7
- Cañado LG, Takai K, Enoki T, Endo M, Kim YA, Mizusaki H, Jorio A, Coelho LN, Magalhães-Paniago R, Pimenta MA (2006) General equation for the determination of the crystallite size L_a of nanographite by Raman spectroscopy. *Appl Phys Lett* 88(16):163106
- Edie D (1998) The effect of processing on the structure and properties of carbon fibers. *Carbon* 36(4):345–362
- Minus M, Kumar S (2005) The processing, properties, and structure of carbon fibers. *Jom* 57(2):52–58
- Gupta A, Harrison I (1996) New aspects in the oxidative stabilization of PAN-based carbon fibers. *Carbon* 34(11):1427–1445
- Gupta A, Harrison I (1997) New aspects in the oxidative stabilization of PAN-based carbon fibers: II. *Carbon* 35(6):809–818

Publisher's Note Springer Nature remains neutral with regard to jurisdictional claims in published maps and institutional affiliations.